Romanian Reports in Physics, Vol. 66, No. 3, P. 746–753, 2014

EXPERIMENTAL SETUP AIMED TO STUDY THE ELECTRICAL IMPEDANCE VARIATIONS OF A PLASMA COLUMN IN A WIDE FREQUENCY RANGE

O.S. STOICAN

National Institute for Laser, Plasma and Radiation Physics,
Atomistilor 409, RO-077125, POB-MG36, Măgurele, Romania, EU
E-mail: stoican@infim.ro

Received June 28, 2013

Abstract. Implementation of a complete system based on the RF bridge principle, able to detect the impedance variations of a physical system under various experimental conditions is reported. To assure a high sensitivity, the bridge unbalance voltage is amplified by means of an electronic circuit operating as a superheterodyne receiver. Integration of the RF bridge in a synchronous detection scheme is described.

Key words: rf bridge, lock-in amplifier, Faraday dark space, plasma rf absorption, superheterodyne receiver.

PACS: 07.50.Qx, 84.30.Le, 52.25.Os

1. INTRODUCTION

Realization of a complete experimental setup containing a RF bridge as main component, aimed to detect the impedance variation of a physical system due to the action of various external fields, is presented. Although it can be adapted easily for a broad class of applications, the said setup has been mainly designed to study resonance effects and absorption of the RF electromagnetic field within the plasma columns in the presence of an external magnetic field. Compared to other solutions which might be used for the same purposes, such as the marginal oscillator for example [1], RF bridge can be operated at low RF electric field levels and in a wide frequency range without to perform significant modifications of the functional blocks [2, 3].

2. SYSTEM DESCRIPTION

2.1. RF BRIDGE

The electrical diagram of the bridge is shown in Fig.1 where TR1 is a wideband RF center tapped transformer (Coilcraft WB2010, [4]). Circuit topology is similar to those of a Blumlein bridge [2, 3]. The bridge is driven by a RF voltage, U_{rf}, at

frequency f_0 delivered by the generator G_1. The secondary winding is segmented into two identical sections by a center tap. The two secondary sections, L_{s1} and L_{s2}, represent two arms of the bridge. The other arms consist of the measurement cell MC and a circuit, comprised of several passive components, characterized by the equivalent impedance Z_e, hereinafter referred to as "balancing network", respectively. Measurement cell is a capacitor bounding between its plates the system under test. Balancing network simulates the electrical equivalent circuit of the absorption cell and its actual topology depends on the particular system under investigation. Bridge is balanced by adjusting the elements of the balancing network, searching the point where the voltage difference between the transformer secondary center tap and ground, U_{M0}, is null. Actually, the electrical equivalent circuit of a certain physical system under any experimental conditions is difficult to be described accurately. Therefore, the structure of the balancing network represents an approximation of the real physical system under test and, in most cases, balancing bridge means achieving conditions for which voltage U_{M0} reaches a minimum.

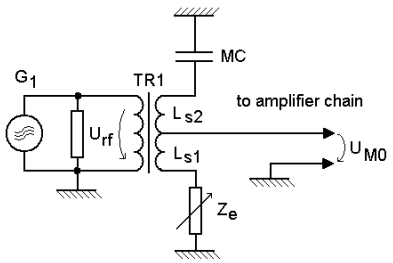

Fig. 1 – Electrical diagram of the bridge. G_1: RF generator, TR1: center tapped wideband transformer, MC: measurement cell, Z_e: balancing network represented by its equivalent impedance

2.2. AMPLIFIER CHAIN

If the electrical equivalent circuit elements of the system under test undergoes are modified as a result of either the changes of its state or action of external fields, then the voltage U_{M0} varies. Because these variations could be very small and buried in noise, it is need to be amplified and filtered. This task is performed by an amplifier chain based on the superheterodyne principle. The advantages of this kind of design, in terms of selectivity, sensitivity and stability, are well known and will be not recalled here (*e.g.* [5]). The block diagram of the amplifier chain is shown in Fig. 2. The core of the mixer stage consists of a NE602 integrated circuit which is represented in Fig. 2 as a dashed box containing several functional blocks [6–8]. According to the data sheet input impedance of the NE602 is 1500Ω. Such a value is relatively low and because of this the input signal can be attenuated. To overcome

this issue, a buffer (denoted as P-A in Fig.2), whose electrical diagram is shown in Fig.3, having input impedance of 10MΩ, is inserted between the transformer secondary center tap and input of the mixer stage. A second RF signal source (denoted as G_2 in Fig.2) accomplishes the function of the local oscillator delivering a RF voltage at frequency f_L. As a rule, output impedance of the modern RF generators is low, usually 50Ω, and output voltage level can be varied over a broad range, so that it is not necessary a buffer stage, the output of generator G_2 being connected only through a capacitor to the NE602 proper terminal. By changing oscillator local voltage level some adjustment of the conversion gain of the mixer can be obtained. Output of the mixer stage is connected to the input of the intermediate frequency amplifier (denoted as IF-A in Fig. 2) whose electrical diagram is shown in Fig.4. In order to

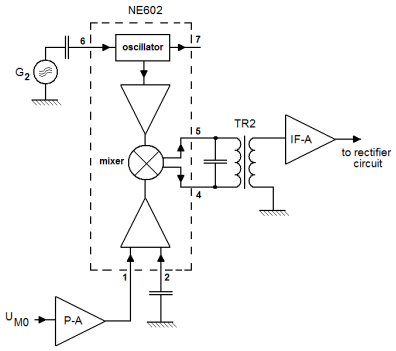

Fig. 2 – Block diagram of the amplifier chain. The functional blocks of the NE602 integrated circuit are contained into dashed box [8]. G_2: RF generator acting as a local oscillator, P-A: buffer, TR2: RF wideband transformer, IF-A: intermediate frequency transformer

improve the common mode rejection, the coupling between NE602 integrated circuit output and IF amplifier input is performed by means of a wideband RF transformer TR2 (Coilcraft WB1010). The IF amplifier is tuned to f_i = 520 kHz. To prevent the

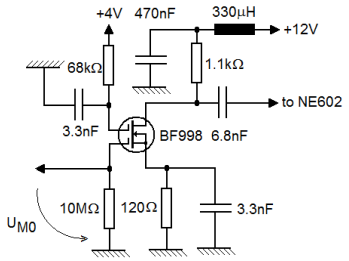

Fig. 3 – Electrical diagram of the buffer (P-A block in Fig.2)

excessive damping of the tuned circuit, IF amplifier output is buffered using a common collector voltage follower stage with high input impedance. To avoid ground loops, another wideband transformer TR3 (Coilcraft WB1010) separates intermediate frequency amplifier from rectifier circuit. The difference $f_0 - f_L$ between output

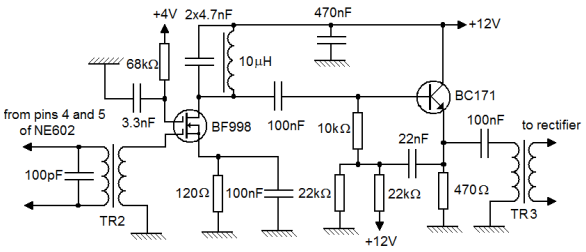

Fig. 4 – Electrical diagram of the intermediate frequency amplifier (IF-A in block in Fig.2)

frequency of the excitation and local oscillators is permanently kept constant, namely equal to intermediate frequency f_i. As a rectifier circuit either an external demodulator (for example a rectifier probe) or a standard rectifier cell implemented on the circuit board can be utilized. As a RF signal source and local oscillator we used Hameg HM8135 and HM8134, respectively [9, 10]. Besides another features, the pieces of equipment mentioned above are able to produce RF sine wave voltage amplitude modulated by an internal generator. The modulation voltage is available at an auxiliary output terminal and it can serve as the reference signal in a synchronous detection scheme. Both RF generators are equipped with interfaces allowing remote control of their operation by means of serial port. Appropriate software was used to settle the output frequencies of RF generators accomplishing the requirement: $f_0 - f_L = f_i$. In this way the RF bridge can operate at various frequencies. The lower and upper limits of the usable frequency band depend on the electrical characteristics of the circuit components and the output maximum frequency of the RF generators. Regardless the features of the external equipment, the electrical characteristics of the electronic circuit components, especially NE602 and RF transformers, must be considered. Thus, for NE602, the maximum input and oscillator frequency are 500MHz and 200 MHz, respectively [8], while the bandwidth of the RF transformers lies between 0.005 and 100MHz [4]. Taking into account the above limitations and constraints related to the intermediate frequency, the operating frequency of the RF bridge lies, theoretically, between 1.5-100MHz. There are applications which do not require the variation of the RF bridge operating frequency. For such purposes a simplified version of the amplifier chain can be built by using possibility of NE602 to operate both as mixer and local oscillator, as it is shown in Fig.5 [8]. To obtain good frequency stability a crystal oscillator topology must be chosen. In the particular case, shown in Fig. 5,

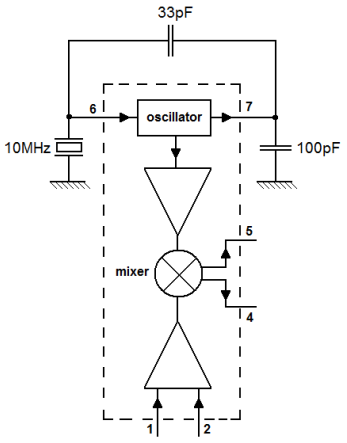

Fig. 5 – 10MHz fixed frequency local oscillator [8]

the RF bridge can operate either at 9.48 MHz or at 10.52 MHz.

2.3. SYNCHRONOUS DETECTION

Output DC voltage of the rectifier, resulting from the intermediate frequency signal demodulation, is a measure of the RF bridge unbalance. Although, for some applications, the sensitivity of the standalone amplifier chain could be good enough, a supplementary filtering of the output signal is necessary for the systems where the noise level is high. For that purpose the RF bridge and amplifier chain are part of a synchronous detection scheme which includes a lock-in amplifier. Consequently, RF excitation voltage applied to the RF bridge is amplitude modulated. The rectified voltage from the amplifier chain output is applied to the input of a lock-in amplifier. For this purpose we used a Standford Research System SR830 lock-in amplifier [11]. As mentioned above, modulation signal is available at the output of the generator G_1 and it is used as a reference signal for the lock-in amplifier. Finally, a multichannel ADC acquisition board records the lock-in output voltage simultaneously with other experimental parameters, allowing tracing the impedance variation of the system under various experimental conditions. The block diagram of the whole setup is shown in Fig. 6.

3. EXPERIMENTAL TESTS

To evaluate the sensitivity limited by the internal noise of the complete setup, the transformer TR1 has been removed and replaced by a 50Ω resistor. RF input voltage has been applied directly to the buffer P-A input. The aim was to determine

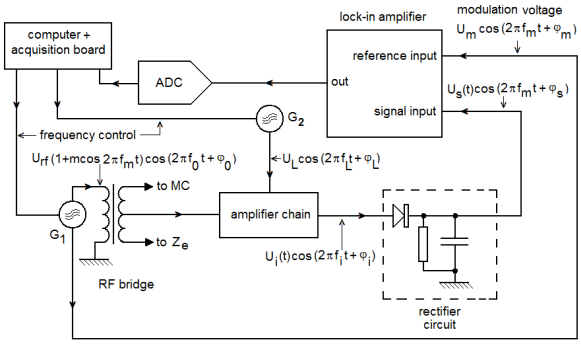

Fig. 6 – Block diagram of the whole setup. G_1: amplitude modulated RF generator, G_2: local oscillator, ADC: analogue to digital converter, MC: measurement cell, Z_e: balancing network

minimum input voltage U_{M0} so that the output signal can be recognized from noise. For a $SNR \simeq 10$dB, at f_0=10 MHz, f_L=10.52 MHz, without amplitude modulation of the input signal, by measuring only amplitude of the signal at IF-A block output, the minimum level of the input voltage was about 3μV. By using the complete setup as it is drawn in Fig. 6 the minimum level of the input voltage has been found about 120 nV (Fig. 7). RF level input represents the value as it is read on the synthesizer HM8135 display [9, 10]. As an application example, in Fig. 8 is shown the RF

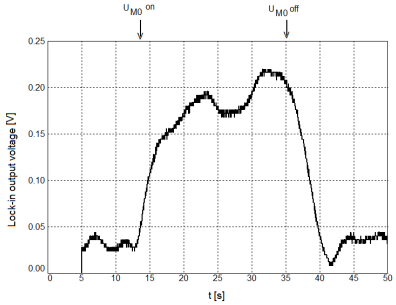

Fig. 7 – Output signal of the lock-in amplifier when input signal U_{M0} is switched on/off. Input signal characteristics: U_{M0} level 120 nV, modulation frequency f_m= 500 Hz, modulation index 100%, lock-in characteristics: sensitivity 20 μV, time constant 1 s, slope/octave 24 dB.

impedance variation of the Faraday dark space region [12–14] of a dc glow discharge as a function on magnitude of an external magnetic field, recorded by using above RF bridge [15]. Measurement cell consists of two external metallic sheets, (X_1, X_2) representing the two halves of a cylinder longitudinally sectioned, placed outside of the discharge tube and coaxially with it (Fig.9a). The presumed equivalent circuit is shown in Fig. 9b. In this application, the magnitude of the impedance variation was fairly large and it was not necessary to utilize synchronous detection methods.

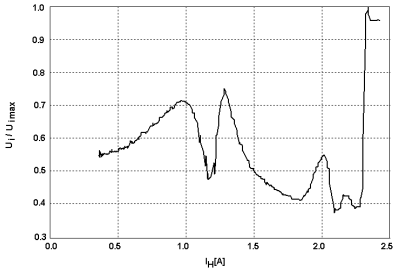

Fig. 8 – RF impedance relative variation of the Faraday dark space region of a dc glow discharge in air at low pressure as a function on generating magnetic field coils current I_H. Experimental conditions: air pressure 6 x 10^{-3} mbar, f_0=30.527 MHz.

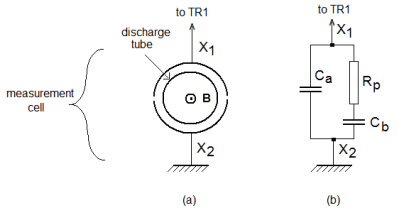

Fig. 9 – (a) Geometrical configuration of the measurement cell; (b) Electrical equivalent circuit of the physical system under test. A similar circuit forms balancing network.

4. CONCLUSIONS

An experimental arrangement intended, especially, to observe variations of the RF impedance of a plasma column under various experimental conditions, has been built and tested. Both bench trials and measurements on the various regions of plasma columns have been performed. Firstly, we achieved a system operating in a wide range of frequency, at a low RF voltage level, able to detect weak RF signals in a possible noisy environment. Secondly, the system architecture was chosen so that to be easily interfaced with a personal computer in order to automatize the change its operating regime and the experimental data acquisition. The above described system allowed us to study the impedance variation of the Faraday dark space region of a dc glow discharge as a function on the magnitude of an external magnetic field [15]. Because the other elements of the complete experimental setup, magnetic field source and high voltage power supply as examples, are also computer controlled, different experimental scenarios could be implemented in a simple manner.

Acknowledgements. This work is done in the framework of the project PN 09 39 03 01 (contract 39N / 2009).

REFERENCES

1. P.A. Probst, B. Collet, W.M. MacInnes, *Rev. Sci. Instrum.*, **47**, 1522-1526 (1976).
2. A.K. Ghosh, *Introduction To Measurements And Instrumentation* (2nd edn. Prentice-Hall of India, New Delhi, 2007 p. 327).
3. D.V.S. Murty, *Transducers And Instrumentation* (2nd edn. PHI Learning Private Limited, 2011, p.99).
4. Coilcraft Inc., *Document 116-1*, Revised 04/22/13, http://www.coilcraft.com
5. J.B. Hagen, *Radio-Frequency Electronics: Circuits and Applications* (Cambridge University Press, 1996).
6. J.J. Carr, *Elektor Electronics*, pp. 20-25, January 1992.
7. D. Anderson, Application note *AN1982*, Philips Semiconductors, December 1991.
8. Philips Semiconductors, Datasheet *SA602 Double-balanced mixer and oscillator*, 07 Nov 1997.
9. Hameg Instruments, Manual *3 GHz RF-Synthesizer HM8135*.
10. Hameg Instruments, Manual *1.2 GHz RF-Synthesizer HM8134-3*.
11. Stanford Research Systems, *Model SR830 DSP Lock-In Amplifier*, Revision 2.3 (12/2006).
12. H. Conrads, M. Schmidt, *Plasma Sources Sci Technol.*, **9**, 441-454 (2000).
13. A. Bogaerts, R. Gijbels, *Spectrochimica Acta*, Part **B 53**, 1-42 (1998).
14. M. Mankour, A. W. Belarbi, K. Hartani, *Romanian Reports in Physiscs*, **65**, 230-245 (2013).
15. O.S. Stoican, *Measurements on the RF impedance variation of the Faraday dark space due to an external magnetic field*, 16th International Conference on Plasma Physics and Applications, June 20-25, 2013, Magurele, Bucharest, Romania, Book of Abstracts, p.86 .